

Coupled-Channel Amplitudes: Physical Effects and Analytic Structure*

EARLE L. LOMON

Laboratory for Nuclear Science and Physics Department, Massachusetts Institute of Technology,
Cambridge, Massachusetts 02139

(Received 15 September 1969)

An investigation is made of the effects of an indefinite number of coupled channels on two-particle amplitudes. Central coupling, chain coupling, and combinations of them are considered. Some results are general, while others depend on a generalized potential model. The existence of strong resonance-producing effects is related to zeros of the S matrix. Forms of Levinson's theorem are found for both the amplitude and S -matrix phases. It is shown that if the effective number of coupled channels increases linearly with the energy that (1) the partial-wave S matrix can vanish asymptotically (the usual result is that $S_L \rightarrow 1$); and (2) Regge trajectories rise asymptotically as the square root of the energy. Special results of the MacDowell symmetry are noted for a finite number of coupled channels. With respect to a special (boundary condition) model it is found that Regge trajectories which cross the origin near $L = \frac{1}{2}$ should have much larger slopes than those crossing the origin near $L = 1$, in agreement with observation. Regge cuts result from the coupling of effective three-body channels.

I. INTRODUCTION

SEVERAL investigations have been made of the effects of interchannel coupling on the analytic properties of scattering amplitudes. In addition to discussion of the inelastic branch points¹ it has been shown that zeros are introduced on the physical sheet² and that asymptotic behavior is affected.³ Important experimental features in one channel may be due to its coupling to other channels. Some resonances have been attributed to the attraction contributed by *closed* channels,⁴⁻⁸ while coupled-channel models are naturally suggested by very inelastic resonances.^{9,10} The majority of calculations of strong interactions among elementary particles have ignored interchannel coupling. The reason for so doing has sometimes been a conjectured dispersion relation for phase shifts.^{11,12} This paper demonstrates the generality of the strongly energy-dependent, often resonance-producing, effects of strongly coupled channels. It explores the effects of coupling on the analytic structure of amplitudes, showing how the physical effects of coupling have been underestimated by conjectured dispersion relations, and detailing the effects on zeros, poles, branch points, and asymptotic behavior in the complex energy and angular momentum planes.

Several qualitative features are demonstrated in a general way. Our quantitative results depend largely on a simple model which has previously been shown to conform to the important features of strong interactions,¹³ including multichannel unitarity and analyticity in the finite-energy plane.

In Sec. II the strongly energy-dependent effect of a coupled channel is shown to extend through the major part of the region between elastic and inelastic thresholds. Only the dispersion relations for amplitudes and some empirical features of the mass spectrum are used in establishing this result. This implies that a strongly coupled channel may easily cause a resonance (or a bound state) far below its threshold, not only an inelastic resonance above its threshold. This is a much more general mechanism than that of Dalitz and Tuan⁴ which depends on the two particles in the higher-mass coupled channel having sufficient attraction between them to bind them in the absence of the lower-mass channel.

In Sec. III we review the basic equations of the model which we will use here to illustrate the qualitative features and to obtain quantitative predictions. The full boundary-condition model (BCM), from which the present model is taken, has been shown to contain a representation of the usually assumed features of quantum-relativistic particle theory.¹³ More important, reason was given for expecting that the simplification of energy-independent boundary conditions closely approximated the results of very strongly interacting particles. At least in one case¹⁴ agreement with data has been sufficiently detailed to substantiate the adequacy of the BCM with field-theoretical potential tails internally bounded by energy-independent boundary conditions. At times we make the further simplification of neglecting the potential tails, thereby ignoring the unphysical cuts in the amplitude. We will refer to

* Work supported in part by the U. S. Atomic Energy Commission under Contract No. AT(30-1)2098.

¹ E. Wigner, Phys. Rev. **73**, 1002 (1948); M. Nauenberg and A. Pais, *ibid.* **126**, 360 (1962). See also Ref. 23, pp. 528-543.

² James B. Hartle and C. Edward Jones, Ann. Phys. (N. Y.) **38**, 348 (1966).

³ R. E. Kreps and P. Nath, Phys. Rev. **148**, 1436 (1966).

⁴ R. H. Dalitz and S. F. Tuan, Ann. Phys. (N. Y.) **10**, 307 (1960).

⁵ L. F. Cook, Jr., and B. W. Lee, Phys. Rev. **127**, 283 (1962); **127**, 297 (1962).

⁶ H. Goldberg and E. L. Lomon, Phys. Rev. **134**, B659 (1964).

⁷ Hyman Goldberg, Phys. Rev. **154**, 1558 (1967).

⁸ E. L. Lomon and A. I. Miller, Phys. Rev. Letters **21**, 1773 (1968).

⁹ M. Krammer and E. Lomon, Phys. Rev. Letters **20**, 71 (1968).

¹⁰ H. Goldberg and E. L. Lomon, Phys. Rev. **131**, 1290 (1963).

¹¹ J. S. Ball and W. R. Frazer, Phys. Rev. Letters **7**, 204 (1962).

¹² A. Donnachie and J. Hamilton, Ann. Phys. (N. Y.) **31**, 410 (1965), especially p. 434.

¹³ H. Feshbach and E. L. Lomon, Ann. Phys. (N. Y.) **29**, 19 (1964).

¹⁴ Earle L. Lomon and Herman Feshbach, Ann. Phys. (N. Y.) **48**, 94 (1968).

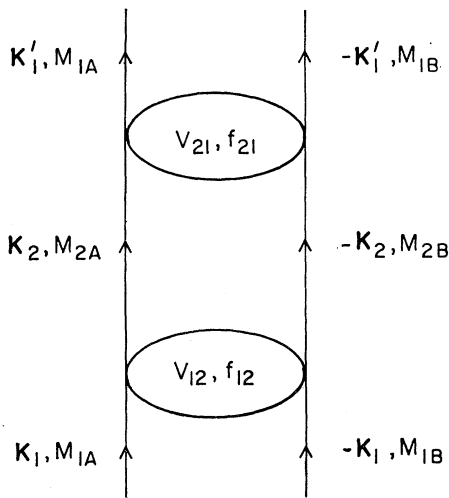


FIG. 1. Lowest-order effect of a coupled channel on elastic scattering. V_{12} and f_{12} represent the interchannel coupling potential and boundary condition.

this version as the SBCM, or simple BCM. Many results are obtained with the inclusion of a diagonal potential matrix, where only the interchannel coupling potential tails are being ignored. This we refer to as the SIBC. The energy-independent matrix boundary conditions (acting on many-channel wave functions) alone can give a good representation of the elastic and inelastic physical cuts. While the omission of the potential must considerably effect quantitative results, especially at low energy, the SBCM has been shown to represent some multichannel systems very well at low and intermediate energies.^{6-10,15,16} At high energies the potential tail will decrease in importance relative to the boundary condition. We expect that the SBCM is a good approximation for the present purpose of investigating the effect of inelastic thresholds at intermediate and high energies. Section III reviews the implementation of the SIBC for an indefinite number of coupled two-particle channels. More than two particles in a channel are handled in the quasi-two-particle approximation in which at least one of the two particles is unstable, and consequently has a mass distribution.

For a finite number of channels the energy-independent BCM predicts exponential asymptotic behavior of amplitudes, although Mandelstam behavior is obtained in finite regions. In Sec. IV we show that Mandelstam behavior at infinity for partial-wave amplitudes may be restored if an infinite number of channels are coupled provided the effective density of thresholds increases linearly in the asymptotic region. It is further shown that in this case it is the partial-wave S matrix which vanishes asymptotically, rather than the partial-wave amplitude vanishing as in other models.³

¹⁵ H. Goldberg and E. L. Lomon, *Nuovo Cimento* **37**, 953 (1965).

¹⁶ E. L. Lomon and C. L. Yen, *Bull. Am. Phys. Soc.* **8**, 21 (1963).

In Sec. V the appearance of a CDD pole¹⁷ with each new coupled channel is noted. Each CDD pole is shown to cause a pole and a zero in the amplitude. The resulting version of Levinson's theorem¹⁸ is described. It is also noted that complex CDD poles are obtained in a channel which is coupled to another channel, which in turn is coupled to a third channel.

Zeros are also produced on the physical sheet of the S matrix. This has important consequences for the formulation and use of dispersion relations for phase shifts. These consequences are shown in Sec. V to invalidate earlier conclusions concerning the weak effect of inelasticity.¹²

Section VI investigates MacDowell symmetry^{15,19} in the SIBC and shows that it is sensitive to the inelastic cuts. Certain simple relations among the amplitudes on which MacDowell symmetry is imposed are found to hold above inelastic threshold.

The behavior of Regge-pole trajectories in the single-channel SBCM has been previously explored.²⁰ The behavior in a coupled-channel SBCM is analyzed in Sec. VII. The slope at threshold predicts the qualitative difference of the Pomeranchon slope from that of the other leading trajectories. The most interesting feature is the asymptotic behavior under the conditions of infinitely many channels derived in Sec. IV. Under this condition the Regge-pole trajectories are shown to rise at the rate of (total energy)^{1/2} (rather than quadratically as extrapolated from present data). The imaginary part increases at the same rate as the real part.

While two-particle channels lead only to poles in the l plane, it is shown in Sec. VII that cuts appear when three-particle channels are included. The slope of the branch points' trajectories at zero total energy is examined and is found to decrease to zero with increasing threshold mass of the three-particle channel. The slopes of the branch-point trajectories therefore accumulate at zero, at momentum transfer squared $t=0$ when one considers crossed-channel amplitudes. This implies an asymptotically constant diffraction peak width and total cross section, consistent with present evidence. It is conjectured that accumulation of these branch points may represent the effects usually attributed to the Pomeranchon trajectory.

Finally, in Sec. VIII, we summarize the results of this paper.

II. DIRECT INELASTIC CONTRIBUTIONS ON THE PHYSICAL CUT

We consider the dispersion relation for a partial-wave amplitude $A_{\alpha L}(s)$, where α represents all the quantum

¹⁷ L. Castillejo, R. H. Dalitz, and F. J. Dyson, *Phys. Rev.* **101**, 453 (1956), hereafter referred to as CDD.

¹⁸ N. Levinson, *Kgl. Danske Videnskab. Selskab, Mat.-Fys. Medd.* **25**, No. 9 (1949).

¹⁹ S. W. MacDowell, *Phys. Rev.* **116**, 774 (1959).

²⁰ V. N. Gribov and I. Ya. Pomeranchuk, *Phys. Rev. Letters* **9**, 238 (1962).

numbers of the channel other than the orbital angular momentum L , and s in the square of the barycentric energy. The inelastic cut due to a channel $\alpha'L'$ with threshold S_i will contribute a term to the dispersion relation

$$\Delta A_{\alpha L} = -\frac{1}{\pi} \int_{s_i}^{\infty} \frac{\rho_{\alpha'L',\alpha L}(s')}{s'-s} ds'. \quad (1)$$

This term arises from the process of Fig. 1, so that by unitarity

$$\rho_{\alpha'L',\alpha L}(s') = |\langle \alpha'L' | \alpha L \rangle|^2, \quad (2)$$

which is *positive definite*. The contribution of Eq. (1) will induce changes in the discontinuities across the unphysical ($s < s_u$) and elastic ($s > s_e$) cuts, effecting higher-order contributions of the coupling to the amplitude. In the physical region the effect on the amplitude of the alteration in the unphysical cut is small and, because of the separation of the regions, its effect on energy dependence is even smaller. The change in discontinuity on the elastic cut is just the effect in which we are interested. This change in the elastic discontinuity can modify but not cancel the effect of Eq. (1), because then the change would itself be cancelled. It follows that the behavior of ΔA in the physical region is a measure of the effect of the coupled channel.

The threshold behavior of the production amplitude $\langle \alpha'L' | \alpha L \rangle$ leads immediately to the expected cusp in $A_{\alpha L}$ at inelastic threshold.^{1,6} We shall not repeat that simple analysis here. However, the amplitude of the cusp is not large; thus it is an unimportant physical characteristic, difficult to discern with available resolution. The contribution $\Delta A_{\alpha L}$ of Eq. (1) contains other, much more important, effects over large energy ranges. The most obvious is the onset of inelasticity, but the most important is *below* threshold.

When $s < s_i$, the denominator of the integrand in Eq. (1) is positive definite, so that $\Delta A_{\alpha L}$ is *always attractive*. Furthermore, as s approaches s_i from below, the denominator decreases for all s' , so that $\Delta A_{\alpha L}$ grows as threshold is approached. The increasing attraction so induced in the partial wave by the higher-threshold coupled channel is characteristic of a resonance amplitude. If the numerator is of normal strong-interaction magnitude a resonance of moderate width may well occur,^{5-8,16} depending on the amount of attraction or repulsion in the background terms. It should be noted that this resonance mechanism does not depend on attraction in the higher-mass channel (acting as in Fig. 2) such that the channel would be bound in the absence of its coupling to the lower-mass channel. The latter mechanism⁴ produces a narrow resonance near the energy at which the bound state would have appeared. Such a quasi-bound-state mechanism, is of course, much more special than the resonance-producing effect discussed above. It has been shown that the general coupled-channel mechanism is sufficient to produce the

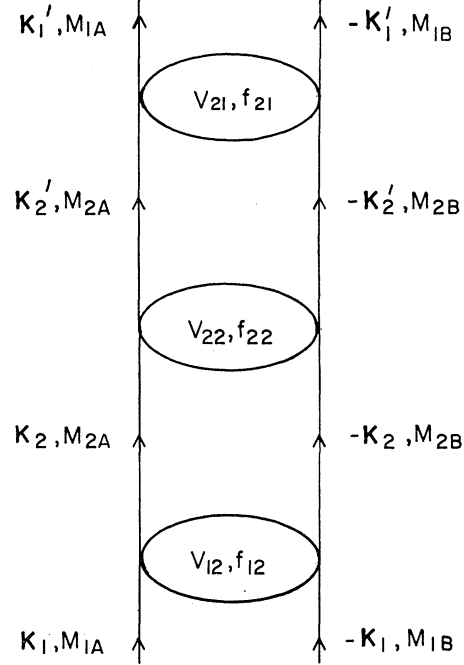


FIG. 2. Lowest-order effect of diagonal interaction in the secondary channel. V_{12} and f_{12} represent the interchannel coupling potential and boundary condition. V_{22} and f_{22} represent the diagonal potential and boundary condition acting in the intermediate-state channel.

$Y_0^*(1405)$ resonance^{13,16} without invoking the quasi-bound effect for that resonance.⁴

If most of the contribution to the integrand of Eq. (1) is from near inelastic threshold, the energy dependence of $\Delta A_{\alpha L}$ is as fast as $(s-s_i)^{-1}$. However, $\langle \alpha'L' | \alpha L \rangle$ will, in general, peak at a value of s' determined by the range R of the interaction, such that (with $\hbar=c=1$)

$$(s'-s_i)^{1/2} \approx (2L'+1)R^{-1} = (2L'+1)\mu,$$

where μ corresponds to the mass of the exchange particle determining the range of the production reaction. The energy dependence implied is

$$\Delta A_{\alpha L} \propto [s_i + (2L'+1)^2\mu^2 - s]^{-1}. \quad (3)$$

As expected, the larger the range, the stronger the induced energy dependence.

Given more or less equal strong-interaction weight functions, the contribution $\Delta A_{\alpha L}$ will become more important in the elastic region than the contribution of the unphysical cut (exchange force) when

$$s - s_u > s - [s_i + (2L'+1)^2\mu^2], \quad (4)$$

where s_u is the threshold of the unphysical cut ($s_u < s_e$). It follows that the inelastic contribution is likely to be important in the range from about s_i down midway between s_e and s_i , and may still be of some importance in the vicinity of elastic threshold s_e .

We remark that the form of Eq. (1) can easily be understood in perturbation theory. If $\langle \alpha'L' | \alpha L \rangle$ is

approximated by a perturbation matrix element (e.g., a simple particle-exchange contribution) then Eq. (1) reduces to a second-order Born expression, which is well known to be attractive in the elastic region. Similarly, higher-order terms in the Born series expansion of Eq. (1) representing iterations of Fig. 1 are of even order in the transition matrix element, leading to attraction.

III. MODEL

In Ref. 13 it is shown that the Schrödinger amplitude generated by a superposition of Yukawa potentials and a homogeneous boundary condition at a core radius r_0 is a general representation of relativistic amplitudes with the normal singularities in the finite-energy plane. The boundary condition need have at most real poles of positive residue in the energy plane (a generalization of the Wigner causality condition) and in this form defines the BCM. It was further shown in Ref. 13 that strong contributions from the double-spectral-function region closest to the s axis (in the st plane, where t is the momentum transfer squared) tend to make the boundary condition *energy-independent*. This part of the spectral function begins at values of t corresponding to two-particle exchange, so that the boundary condition is expected to approach energy independence at the equivalent interaction radius. The BCM is usually applied in its energy-independent form to strong interactions.

If the energy-independent form is to be appropriate in the case of strongly coupled channels, it is necessary to use matrix potentials and boundary conditions of a dimension sufficient to include the important channels. This coupled-channel form may be reduced to a one-channel equation by elimination of the other amplitudes, leading to an energy-dependent interaction term.^{6-10,16} This term generates the amplitude dependence discussed in Sec. II, explicitly introducing new singularities and zeros into the amplitude.

The potential of the BCM, which may be deduced^{14,21} or at least restricted²² theoretically, is the appropriate long-range part of strong interactions. As such, it is important to the energy dependence at low energies, and to the angular dependence at small angles. However, its effect is unimportant asymptotically with energy, and it adds no new features at inelastic thresholds, the two main regions of interest in the present investigation. For the sake of obtaining simple quantitative results we will sometimes ignore the potential tail and use only the constant matrix boundary conditions, the SBCM. However, our analytical results follow without complication if the diagonal part of the potential matrix does not vanish. When only the *interchannel* potentials are

assumed to vanish, the nomenclature SIBCM will be used.

In the BCM the amplitude Ψ is defined by

$$r_0 d\Psi/dr_0 = \mathfrak{f}\Psi(r_0). \quad (5)$$

$\Psi(r)$ is a column matrix with components $u_{\alpha_i L_i}(r)$, functions of the two-particle separation r , and \mathfrak{f} is a square matrix with constant, real symmetric, components f_{ij} . The indices i, j , run over the N channels whose coupling is important to the energy dependence of a certain reaction in some energy region. Channels with distant thresholds will only renormalize the constants f_{ij} of low-mass channels. The $u_{\alpha L}(r)$, $r > r_0$, are the radial wave functions in the external potential. It follows that in the SIBCM, for $r > r_0$,

$$U_{\alpha L}(r) = A_{\alpha L} J_{L^-}(K, r) + B_{\alpha L} J_{L^+}(K, r), \quad (6)$$

where J_{L^-} and J_{L^+} are, respectively, the incoming and outgoing Jost functions²³ in the diagonal potential $V_{\alpha L}$, K is the relativistic relative momentum in the channel, and the $A_{\alpha L}$, $B_{\alpha L}$ are to be determined by Eq. (5) and experimental conditions concerning incoming and outgoing channels. In the SBCM, $V_{\alpha L} = 0$ and we have

$$J_{L^-}(K, r) = r h_L^{(2)}(Kr), \quad J_{L^+}(k, r) = r h_L^{(1)}(Kr), \quad (7)$$

where the $h_L^{(1)}$ and $h_L^{(2)}$ are the spherical Hankel functions.

The $\alpha_i L_i$ will be connected by strong selection rules. The combination of threshold positions and selection rules will usually lead to only two or three channels being of importance in a finite-energy application. As one would expect, one must consider an infinite number of channels to obtain the asymptotic energy behavior. The introduction of new singularities at finite energies may be studied by the addition of one new channel at a time.

If the incoming channel is designated by $i=1$, then the S matrix in the SIBCM is defined by

$$U_{\alpha_1 L_1}(r) = K_1^{-1/2} [J_{L_1^-}(K_1, r) + S_{11} J_{L_1^+}(K_1, r)] \quad (8)$$

and

$$U_{\alpha_i L_i} = K_i^{-1/2} S_{1i} J_{L_i^+}(K_i, r), \quad i=2, \dots, N \quad (9)$$

where the channel momenta K_i ($i=1, \dots, N$) are fixed by the total energy W and the channel masses M_{iA} and M_{iB} (particles A and B , respectively),

$$W = (K_i^2 + M_{iA}^2)^{1/2} + (K_i^2 + M_{iB}^2)^{1/2}. \quad (10)$$

The flux normalization factor $K_i^{-1/2}$ together with the symmetry and reality of the \mathfrak{f} matrix ensure the unitarity of the S matrix; i.e., above elastic threshold,

$$\sum_{i=1}^N |S_{1i}|^2 = 1. \quad (11)$$

This is proven in the Appendix.

²³ Roger G. Newton, *Scattering Theory of Waves and Particles* (McGraw-Hill Book Co., New York, 1966), p. 334, footnote.

²¹ M. H. Partovi and E. L. Lomon, *Phys. Rev. Letters* **22**, 438 (1969); M. H. Partovi, thesis, M.I.T., 1969 (unpublished).

²² W. W. S. Au and E. L. Lomon, *Nuovo Cimento* **31**, 113 (1964).

(a) For the two-coupled-channel system the matrix equation (5) represents two coupled equations. In the SIBCM, using Eq. (9), the second of those coupled equations leads algebraically to

$$K_2^{-1/2}S_{12} = \frac{f_{12}U_{\alpha_1 L_1}(r_0)}{r_0(d/dr_0)[J_{L_2}^+(K_2, r)] - f_{22}J_{L_2}^+(K_2, r_0)}. \quad (12)$$

Equation (12) can then be substituted into the first of the coupled equations to give

$$r_0 dU_{\alpha_1 L_1}/dr_0 = f_{\text{eff}}U_{\alpha_1 L_1}(r_0), \quad (13)$$

with

$$f_{\text{eff}} = f_{11} - \frac{f_{12}^2}{f_{22} + \theta_2^+(K_2)}, \quad (14)$$

where

$$\theta_i^\pm(K_i) = -\frac{r_0}{J_{L_i}^\pm(K_i, r_0)} \frac{dJ_{L_i}^\pm(K_i, r_0)}{dr_0}. \quad (15)$$

Inserting Eq. (8) into Eq. (13), one solves for

$$S_{11} \equiv \eta_{11} e^{2i\delta} = \frac{f_{\text{eff}} + \theta_1^-(K_1) J_{L_1}^-(K_1, r_0)}{f_{\text{eff}} + \theta_1^+(K_1) J_{L_1}^+(K_1, r_0)}. \quad (16)$$

The Jost functions required are calculated by integration of the Schrödinger equation from their asymptotically defined values to r_0 with the diagonal potential appropriate to the channel.

The analytic properties of the Jost functions—and therefore of the θ_i^\pm functions—are well known²³ provided the potential is a superposition of Yukawa potentials. Branch points are present in $J_{L_i}^\pm$ at $K_i = \mp \frac{1}{2}iM_e$, where M_e is the smallest “exchange mass” represented by the Yukawa-potential distribution. Zeros of the $J_{L_i}^+$ (and therefore poles of the θ_i^+) exist only for $\text{Re}K_i = 0$ or $\text{Im}K_i < 0$. A zero at $\text{Re}K_i = 0$, $\text{Im}K_i > 0$ represents a bound state of the i th channel at the pole if $f_{ii} \rightarrow \infty$. (This is the same as a hard-core potential at r_0 . In known cases the potential beyond r_0 is not sufficiently attractive to bind.) If f_{ii} is finite, then a more deeply bound state or Dalitz-Tuan resonances in other channels are induced by such a pole. Poles at $\text{Im}K_i < 0$ may produce resonances in the i th channel.

For our purposes the important properties of the Jost functions are

$$J_{L_i}^+(K_i, r_0) = J_{L_i}^-(-K_i, r_0) \quad (17)$$

and

$$J_{L_i}^{\pm*}(-K_i^*, r_0) = J_{L_i}^\pm(K_i, r_0). \quad (18)$$

Equation (18) establishes that $J_{L_i}^\pm$ and therefore the θ_i^\pm , are real when K_i is imaginary. Equation (17) shows that the S_{11} of Eq. (16) has modulus unity when K_1 is real and f_{eff} is real; according to the above reality condition and Eq. (14), the reality of f_{eff} is assured when K_2 is imaginary, leading to the expected $S_{11}^* = S_{11}^{-1}$ between elastic and inelastic threshold.

Above inelastic threshold the sign of $\text{Im}\theta_i^\pm$ is important to unitarity, and can be easily established by using the asymptotically evaluated Wronskian

$$W[J_{L^+}, J_{L^-}] \equiv J_{L^+}(K, r_0) \frac{d}{dr_0} J_{L^-}(K, r_0) - J_{L^-}(K, r_0) \frac{d}{dr_0} J_{L^+}(K, r_0) = -2iK, \quad (19)$$

from which

$$-\frac{r_0 W}{J_{L^+} J_{L^-}} = \theta_{L^-} - \theta_{L^+} = \frac{2iK r_0}{J_{L^+} J_{L^-}}. \quad (20)$$

Using Eqs. (17) and (18) we have

$$J_{L^-}(K, r) = [J_{L^+}(K, r)]^* \quad \text{for } K \text{ real} \quad (21)$$

and a similar result for the θ^\pm functions, so that Eq. (20) becomes

$$\text{Im}\theta_{L^+} = \frac{-K}{|J_{L^+}|^2} \leq 0, \quad K \text{ real}. \quad (22)$$

Similarly,

$$\text{Im}\theta_{L^-} \geq 0, \quad K \text{ real}. \quad (23)$$

Applying Eq. (22) to θ_2^+ we have from Eq. (14)

$$\text{Im}f_{\text{eff}} \leq 0. \quad (24)$$

Because of their signs,

$$|\text{Im}(f_{\text{eff}} + \theta_1^-)| \leq |\text{Im}(f_{\text{eff}} + \theta_1^+)|, \quad (25)$$

so that Eq. (16) leads to

$$|S_{11}| \leq 1, \quad K_2 \text{ and } K_1 \text{ real}. \quad (26)$$

The above unitarity property is proven for the general case in the Appendix, but we have seen directly how it arises in the SIBCM from the reality properties of Jost functions.

Because the threshold properties ($K_i \rightarrow 0$) of the Jost functions are similar to those of the Hankel functions, $\theta_{L^+}(Kr_0) \sim (Kr_0)^{2L+1}$, the elastic and inelastic threshold properties of S_{11} follows from Eq. (16) in the same way as in the Appendix of Ref. 10.

We now turn to the distribution of S -matrix poles in the SIBCM. If at a pole of S_{11} , integration of the Schrödinger equation for the first channel would lead to Eq. (3.18) of Ref. 13, which *excludes*, when $\text{Im}K_1 \geq 0$,

$$(\text{Im}f_{\text{eff}}/\text{Re}K_1) \leq 0. \quad (27)$$

Thus if $\text{Im}f_{\text{eff}} < 0$ there are no poles of the S matrix for $\text{Im}K_1 \geq 0$ unless $\text{Re}K_1 = 0$. The f_{eff} of Eq. (14) can easily be seen to satisfy Eq. (27) for $\text{Im}K_1 = 0$ because f_{eff} is real below the inelastic threshold, and satisfies Eq. (24) above inelastic threshold. The satisfaction of Eq. (27) by f_{eff} can now be extended to the whole physical sheet ($\text{Im}K_1 > 0$ and $\text{Im}K_2 > 0$) by the properties of the decoupled second channel. The expres-

sion $(f_{22} + \theta_2^+)$ in f_{eff} would be the denominator of S_{22} if $f_{12} \rightarrow 0$. Because f_{22} is a real constant the results of Ref. 13 apply and $(f_{22} + \theta_2^+)$ cannot have a zero for $\text{Im}K_2 > 0$ unless $\text{Re}K_2 = 0$. This implies that $\text{Im}\theta_2^+$ cannot have a zero unless $\text{Re}K_2 = 0$, since otherwise one could choose f_{22} so as to satisfy $(f_{22} + \text{Re}\theta_2^+) = 0$ at the zero of $\text{Im}\theta_2^+$. Consequently, starting from positive (negative) values of K_2 and going throughout the first (second) quadrant of the K_2 plane, $\text{Im}\theta_2^+$ has the same sign as on the real axis. Therefore $(\text{Im}\theta_2^+/\text{Re}K_2) < 0$ when $\text{Im}K_2 \geq 0$ and $\text{Re}K_2 \neq 0$. This implies that Eq. (27) is satisfied, sufficient to disallow unphysical poles of S_{11} .

We now turn to the quantitative behavior of the poles of S_{11} . Since this depends on the details of the potential tail, we begin with the SBCM and then consider the modification caused by a potential. In the SBCM the Jost functions are expressed as Hankel functions [Eq. (7)] and $\theta_i^\pm \rightarrow {}^H\theta_i^\pm$. Well-known properties of the Hankel functions at threshold ($K_i = 0$) give

$${}^H\theta_i^+(0) = L_i \quad (28)$$

and for $k = i\chi$, $\chi > 0$,

$$\frac{d}{d\chi} [{}^H\theta_i^+(K_1 r_0)] > 0 \quad (29)$$

because $iyh_L^{(1)}(iy) = i^{-L-1}S_L(y)e^{-y}$, where $S_L(y)$ is a polynomial in y^{-1} with positive coefficients. These equations show that f_{eff} has at most one pole for $\chi_L > 0$, and that only if $f_{22} \leq -L_2$. If $f_{22} = -L_2$ the pole is at threshold, and then the pole moves to larger χ_2 as f_{22} decreases. Such a pole in f_{eff} is often called a "quasi-bound" state, because the second channel would be bound at that χ_2 if $f_{12} \rightarrow 0$. Equation (16) shows that a pole of S_{11} will occur in the vicinity of a pole in f_{eff} (how near depends on the f_{12} which determines the residue of the pole in f_{eff}). The pole in S_{11} will either be just below the real K_1 axis leading to a resonance in the first channel (the Dalitz-Tuan mechanism⁴) or, if the value of χ_2 at the pole in f_{eff} is large enough, it will be a true bound state of the first channel.

If an attractive potential tail is present, it will increase the value of χ_2 at which there is a pole, while a repulsive tail will decrease that χ_2 and may remove the pole from the quasi-bound region $\chi_2 > 0$. If the potential is sufficiently attractive to bind channel 2 with a hard core at r_0 it will cause a pole in $\theta_2^+(K_2, r_0)$ for $\chi_2 > 0$, thus inducing a pole in f_{eff} and S_{11} in that region—another source of the Dalitz-Tuan quasi-binding. Similarly, one would have n or $n+1$ poles in f_{eff} when there are n poles of $\theta_2^+(K_2, r_0)$ for $\chi_2 > 0$. More than $n+1$ poles in f_{eff} would imply an oscillation of θ_2^+ along the imaginary K_2 axis. The oscillation of θ_2^+ would cause "bound-state" poles of the wrong signature in S_{22} (uncoupled) unless the numerator of S_{22} provides compensating changes of sign. Since S_{22} has been shown to be free of disallowed singularities, this would restrict the number

of poles of f_{eff} to $n+1$ except under unusual circumstances. We have not investigated to see if these unusual circumstances exist.

Having established the strongly attractive, strongly energy-dependent effect of the Dalitz-Tuan mechanism when $(f_{22} + \theta_2^+)$ has a zero for $\chi_2 > 0$, we now confirm that strongly energy-dependent attractive effects persist when there is no such zero, as predicted more generally in Sec. II. For $\chi_2 > 0$ in the SBCM,

$$f_{\text{eff}} = f_{11} - \frac{f_{12}^2}{f_{22} + {}^H\theta_2^+(K_2, r_0)}. \quad (30)$$

If $f_{22} > -L_2$ (so that f_{eff} has no poles on the physical sheet) the denominator in Eq. (30) is positive and increasing with χ_2 due to the monotonic properties of ${}^H\theta_2^+$. It follows that $f_{\text{eff}} < f_{11}$, i.e., more attractive than the uncoupled first channel, and that this attraction increases as the inelastic threshold ($K_2 = 0$) is approached from below. If

$$f_{11} - \frac{f_{12}^2}{f_{22} + L_2} < -L_1, \quad (31)$$

then there will be a resonance in S_{11} below inelastic threshold (or a bound state of S_{11} if the inequality is large enough). This resonance mechanism is less special than that of Dalitz-Tuan and may easily occur in a strong interaction. The second channel does not have to be quasi-bound and may even be repulsive. Only for very strong repulsion in either channel (f_{22} or $f_{11} \gg L_2$) does it become very unlikely that the inequality (31) will be satisfied by reasonable strong interaction values of f_{12} .

Apart from the resonance condition, Eq. (30) shows that f_{eff} will be strongly energy-dependent provided

$$f_{12}^2/|f_{22}| \gtrsim |f_{11}|.$$

The energy range over which the strong variation takes place is determined by ${}^H\theta_2^+$: Below inelastic threshold it decays exponentially with range $\Delta\chi_2 = r_0^{-1}$, while above inelastic threshold it reaches its maximum at $K_2 \simeq r_0^{-1}(2L+1)$. Since r_0 is determined by the exchange-particle masses, this energy dependence is in agreement with the more general deductions of Sec. II. The addition of potential tails would require that ${}^H\theta_2^+$ be replaced by θ_2^+ in Eq. (30). This would alter the right-hand side of the inequality (31), and lead to small quantitative alterations of the above conclusions.

(b) We now consider N centrally coupled channels. If channels $i=2, \dots, N$ are all coupled to channel 1, but not to each other ($f_{ij} = 0$ unless $i=j$, $i=1$, or $j=1$), we obtain by straightforward elimination of the outgoing channel equations (5) in the SBCM:

$$f_{\text{eff}} = f_{11} - \sum_{i=2}^N \frac{f_{1i}^2}{f_{1i} + \theta_i^+(K_i)}. \quad (32)$$

This represents the direct effect on channel 1 of the opening of an indefinite number of coupled channels. Equation (32) is appropriate for the investigations of asymptotic behavior.

(c) Coupling to an *unstable particle* can be represented by an extension of Eq. (32). One of our coupled channels may be a quasi-two-particle channel in that one of the two particles may be unstable. Apart from an expected weak angular dependence in the many-body phase space, the final state can be parametrized by the isobar (resonance) mass distribution m . We can then simulate the effect of this many-body state^{9,10} as a continuum of two-body states connected to the initial channel. The weight factor $\rho(m)$ is proportional to the high-energy production cross section for the isobar, and is usually given by a Breit-Wigner distribution. Apart from a normalized $\rho(m)$ the interchannel coupling is represented by a constant D such that $f^2(m) = D\rho(m)$. Converting the sum in Eq. (32) to an integral over m , we have

$$f_{\text{eff}} = f_{11} - D \int_{M_t}^{\infty} \frac{\rho(m) dm}{f_{22} + \theta_2^+(K_2(m))}, \quad (33)$$

where M_t is the threshold mass of the decay products of the isobar.

A simple calculation of S_{1m} shows that at high energy [where all other energy dependence is slow compared to that of $\rho(m)$] the production cross section is proportional to $\rho(m)$ as required. At energies close to the inelastic threshold compared to the half-width of $\rho(m)$, the energy dependence of the $\theta_2^+(K_2)$ function, and to a lesser extent of the $\theta_1^{\pm}(K_1)$ functions, will distort the production cross section. Such threshold effects are expected, and have been compared to experiment.^{8-10,24}

(d) We define a set of N *chain-linked channels* as one in which the i th channel is only coupled to channels $(i-1)$ and $(i+1)$. Then Eqs. (5) lead immediately to a continued fraction solution for the effective boundary condition in channel 1, viz.,

$$f_{\text{eff}} = f_{11} - \frac{f_{12}^2}{f_{22, \text{eff}} + \theta_2^+(K_2)}, \quad (34)$$

where

$$f_{ii, \text{eff}} = f_{ii} - \frac{f_{i, i+1}}{f_{i+1, i+1, \text{eff}} + \theta_{i+1}^+(K_{i+1})} \quad (35)$$

ending with

$$f_{NN, \text{eff}} = f_{NN} \quad (36)$$

if there are N channels altogether.

Chains of the above type can clearly be inserted at any point into a centrally coupled system. One need only replace any f_{ii} in Eq. (32) with an $f_{ii, \text{eff}}$ of the type of Eq. (35), provided none of the channels in a chain is the same as a channel represented by another term of Eq. (32). Thus a very large class of coupled-

channel problems can be handled just as one channel, by replacing f_{ii} by an f_{eff} .

IV. ASYMPTOTIC BEHAVIOR OF PARTIAL WAVES IN THE ENERGY PLANE

The single-channel BCM partial-wave amplitudes have Mandelstam-type analyticity in the finite-energy plane but have an essential singularity at infinity.¹³ The asymptotic behavior of the Jost functions guarantees that Eq. (16) gives

$$\lim_{K_1 \rightarrow \infty} S_{11} = (-1)^{L+1} e^{-2iK_1 r_0}. \quad (37)$$

(Note that this differs by a phase of π from the hard-core case.) For any finite number of coupled channels $\lim_{K_1 \rightarrow \infty} f_{\text{eff}} = f_{11}$ [as the $\theta^{\pm} = O(K_1)$ as $K_1 \rightarrow \infty$], so that the asymptotic behavior of S_{11} is unchanged.

This essential singularity can only be avoided for a finite number of coupled channels by making the boundary conditions energy-dependent. The exponential singularity at infinity in Eq. (37) can obviously be avoided if $r_0(K_1) = O(1/K_1)$ as $K_1 \rightarrow \infty$. Alternatively, as discussed in Ref. 13, one may keep r_0 constant but set

$$\lim_{K_1 \rightarrow \infty} f_{11}(K_1) = \lim_{K_1 \rightarrow \infty} (\theta_1^+ J_1^+ - \theta_1^- J_1^-) (J_1^- - J_1^+)^{-1} = -K_1 r_0 \tan K_1 r_0, \quad (38)$$

for instance by Eq. (3.32) of that reference. This will guarantee $\lim_{K_1 \rightarrow \infty} S_{11} = 1$, using Eq. (16). Note that $f_{11}(K_1)$ given in Ref. 13 satisfies the Wigner causality condition $df_{11}/dE_1 \leq 0$.

While the above is possible, Eq. (38) lacks motivation while the asymptotic shrinking of r_0 would beg the question by leaving open the description of the very nonlocal interaction expected at short range. Instead we note here that the opening of more and more channels at high energy (which can always be mediated by medium-range interactions) provides an alternative way of cancelling the essential singularity at infinity. Asymptotically,

$$\text{all } \theta_L^-(K_1 r_0) \rightarrow +iK_1 r_0. \quad (39)$$

Therefore if

$$f_{\text{eff}} \rightarrow -iK_1 r_0, \quad (40)$$

it follows from Eq. (16) that $S_L \rightarrow 0$.

We now seek the coupling conditions that lead to Eq. (40). As we go to higher energy, we may expect the thresholds to become more dense and we may make a continuum approximation to Eq. (32). This will give a result similar to that of Eq. (33) if

$$D\rho(m) \rightarrow f^2(m)\sigma(m), \quad (41)$$

where $\sigma(m)$ represents the density of channel openings and $f(m)$ represents a local average interchannel coupling constant. Asymptotically we then have, when

²⁴ M. Krammer, Nuovo Cimento **53**, 762 (1968); Filippas *et al.*, *ibid.* **51**, 1053 (1967).

$K_1 \gg T \gg M_1$,

$$\lim_{K_1 \rightarrow \infty} f_{\text{eff}} = \bar{f}_{11} - D \int_T^\infty \frac{\rho(m) dm}{f_{22}(m) - ir_0(K_1^2 - m^2)^{1/2}}, \quad (42)$$

where we have used the result $\theta_2^+(K_2) \rightarrow -iK_2 r_0$; and

$$K_2^2 = K_1^2 - (m^2 - m_1^2) \approx K_1^2 - m^2, \quad (43)$$

where $2m$ is the threshold mass, and T represents the value of $2m$ at which our asymptotic assumptions hold. All the thresholds for which $2m < T$ are included in \bar{f}_{11} , which is constant asymptotically. From Eq. (43) we have

$$\begin{aligned} \text{Im} f_{\text{eff}} &= -D \int_T^{K_1} \rho(m) dm \frac{r_0(K_1^2 - m^2)^{1/2}}{f_{22}^2(m) + r_0^2(K_1^2 - m^2)} \\ &\approx -D \int_T^{K_1} \frac{\rho(m) dm}{r_0(K_1^2 - m^2)^{1/2}}, \end{aligned} \quad (44)$$

where we assume $|f_{22}(m)| \ll K_1 r_0$. If we now assume $\rho(m) = r_0 \lambda m$, then

$$\text{Im} f_{\text{eff}} = -D \lambda (k_1^2 - T^2)^{1/2} \rightarrow -D \lambda k_1.$$

Therefore, if we set

$$D \lambda = r_0 \quad \text{or} \quad D \rho(m) = r_0^2 m, \quad (45)$$

then we obtain $\text{Im} f_{\text{eff}} \rightarrow -r_0 K_1$, as required.

With the same assumptions,

$$\begin{aligned} \text{Re} f_{\text{eff}} &= \bar{f}_{11} - \frac{1}{2} r_0^2 \int_{K_1}^\infty \frac{dm^2}{f_{22}(m) + (m^2 - K_1^2)^{1/2} r_0} \\ &\quad - \frac{1}{2} r_0^2 \int_T^{K_1} \frac{f_{22}(m) dm^2}{f_{22}^2 + r_0^2(K_1^2 - m^2)} \rightarrow \ln \frac{k_1 r_0}{f_{22}(\infty)}, \end{aligned} \quad (46)$$

where we have assumed that $f_{22}(m)$ is asymptotically constant and that the divergent first integral in Eq. (46) is absorbed by a renormalization inherent in \bar{f}_{11} . $\text{Re} f_{\text{eff}}$ increases slower than $\text{Im} f_{\text{eff}}$.

Thus if channel couplings effectively increase linearly with K_1 asymptotically, satisfying Eq. (45), we satisfy Eq. (40) and $S_L \rightarrow 0$. This eliminates the bad analytic behavior at infinity and, as we shall see, leads to interesting asymptotic predictions for Regge trajectories.

Although a linear effective increase in channel openings seems reasonable it is certainly not an *a priori* requirement. However, analyticity at infinity imposes a powerful restraint on asymptotic channel coupling in our model. This result provides a counterexample to the conjecture of Ref. 3 (based on strong assumptions about the K matrix) that asymptotically $|S_L| \rightarrow 1$ for the general case, even when there are an infinite number of coupled channels.

V. CDD-TYPE SINGULARITIES

Equations (13), (32), and (35) show that each coupled channel introduces new singularities to f_{eff} . Each pole

in f_{eff} will produce, as is evident through Eq. (16), a pole and a zero of the S -matrix component. Since the amplitude is given by

$$A_1 = (S_{11} - 1)W/2iK_1, \quad (47)$$

the amplitude will also have a pole and a zero related to a pole in f_{eff} . If the residue of the pole in f_{eff} is small, the poles and zeros in S_{11} and A_1 will be nearly on, but not necessarily on, the physical sheet.

The poles of f_{eff} are essentially CDD poles,¹⁷ as discussed below. In this section we shall investigate the distribution of these poles and their appearance with each additional coupled channel. The consequent increment in poles and zeros of the amplitude is studied, leading to a generalized form of Levinson's theorem. Knowledge of the approximate distributions of these poles is valuable in considering the ambiguity in N/D solutions to dispersion relations, or when evaluating the validity of phase-shift dispersion relations. CDD based their study of the ambiguity of solutions to the Chew-Low equation on the properties of Herglotz functions. Wigner and Eisenbud²⁵ had earlier used the Herglotz function properties of the inverse of the reaction (R) matrix for a finite-range interaction. Our \mathfrak{f} matrix is by definition [Eq. (5)] the inverse of the R matrix for the interaction $r < r_0$, and has the necessary Herglotz properties by virtue of Eq. (27) and its reality properties. Thus each pole of the \mathfrak{f} matrix is an example of the ambiguity of the Herglotz functions and it seems appropriate to call them the CDD poles in the present representation. However, because there is an interaction for $r > r_0$, the \mathfrak{f} matrix is not the inverse of the full reaction matrix. Consequently, a pole of f_{eff} is not a zero of the amplitude, as seen in Eq. (16), but instead induces a zero nearby.

In Ref. 17 the Herglotz function used to demonstrate the ambiguity of the Chew-Low equation was also not the actual inverse-reaction matrix, but included the nucleon form factor. Again, when applied to an N/D solution of dispersion equations the term CDD pole has a particular definition—a pole of the D function. The N function is, of course, not the exact equivalent of a form factor. The unifying requirement for the nomenclature CDD pole is that it be a pole of a Herglotz function which enters into the definition of the amplitude. In our case the \mathfrak{f} matrix has the necessary formal properties and has the same physical interpretation as the original model of Ref. 25.

It has long been recognized that multichannel problems lead to poles of the D function^{26,27} of the effective one-channel problem. The definition of the D function then depends on the way in which the inelasticity is put

²⁵ E. P. Wigner and L. Eisenbud, Phys. Rev. **72**, 29 (1947).

²⁶ M. Bander, P. W. Coulter, and G. S. Shaw, Phys. Rev. Letters **14**, 270 (1965).

²⁷ D. Atkinson, K. Dietz, and D. Morgan, Ann. Phys. (N. Y.) **37**, 77 (1966); D. Atkinson and D. Morgan, Nuovo Cimento **41**, 559 (1966).

into the one-channel problem. Of the two methods discussed in the literature, in one $\arg D = -\arg A$ and poles of D correspond to zeros of A .²⁸ In the other, $\arg D = -\frac{1}{2}\arg S$ and poles of D correspond to zeros of S .²⁹ One needs to know how many zeros of A or S are on the physical sheet if one wants an extended Levinson's theorem for $\arg A$ or $\arg S$, respectively. One needs to know that there are no physical zeros of A or S in order to use dispersion relations in A^{-1} or in $\arg S$, respectively, both of which have been considered.

Each pole of f_{eff} (f pole) is associated with a coupled channel. In studying the zeros of A and S associated with an f pole, we are examining the extent of CDD ambiguity in coupled-channel problems of either type discussed above. Our procedure then is to first find the distribution of f poles, then the distribution of S zeros, and lastly the distribution of A zeros. Particular attention is paid to the emergence of zeros onto the physical sheet and their proximity to the physical cut.

(a) Equation (14) is adequate to describe the position of each f pole for any two-particle multichannel model described in Sec. III. The introduction of a channel λ coupled to channel 1 (whose amplitude and S matrix is the one of interest) has an f pole when

$$f_{\lambda\lambda} + \theta_{\lambda}^{+}(K_{\lambda}) = 0. \quad (48)$$

As discussed after Eq. (27) in Sec. III,

$$\text{Im}\theta_{\lambda}^{+}(K_{\lambda}) < 0 \quad \text{when} \quad \text{Im}K_{\lambda} \geq 0, \quad \text{Re}K_{\lambda} \neq 0,$$

whereas $\text{Im}f_{\lambda\lambda} = 0$ if we consider only "centrally coupled" channels [Secs. III(a) and III(b)] or $\text{Im}f_{\lambda\lambda} \leq 0$ if we wish to include the "chain-linked" channels [Sec. III(d)]. In either case, all f poles are on the unphysical sheet unless $\text{Re}K_{\lambda} = 0$. For the centrally coupled cases, any f pole is on the negative $\text{Im}(K_{\lambda})$ axis when $f_{\lambda\lambda}$ is greater than a critical value, but one is on the positive $\text{Im}(K_{\lambda})$ axis when $f_{\lambda\lambda}$ is less than that critical value, f_c . When $\text{Im}f_{\lambda\lambda} < 0$ (chain-linked case), $\text{Im}K_{\lambda} < 0$ and $\text{Re}K_{\lambda} \neq 0$. The condition for a physical f pole is

$$f_{\lambda\lambda} < f_c. \quad (49)$$

As stated after Eq. (29), in the SBCM one obtains $f_c = -L_{\lambda}$. In fact, Eq. (49) is the general condition for a quasi-bound state of the λ channel, causing a resonance in the channel 1. Below we shall see that the satisfaction of inequality (49) makes a qualitative difference to the emergence of physical zeros of A or S .

For convenience we classify the physical sheet, $\text{Im}K_1 > 0$ and $\text{Im}K_{\lambda} \geq 0$, as P and the unphysical sheets as U_1 ($\text{Im}K_1 \geq 0$, $\text{Im}K_{\lambda} < 0$), U_2 ($\text{Im}K_1 < 0$, $\text{Im}K_{\lambda} \geq 0$) and U_3 ($\text{Im}K_1 < 0$, $\text{Im}K_{\lambda} < 0$). We note that the f poles are in P for $f_{\lambda\lambda} \leq f_c$ and are in both U_1 and U_3 when $f_{\lambda\lambda} > f_c$.

(b) When $f_{\lambda\lambda} < f_c$ there is an f pole on the positive $\text{Im}K_{\lambda}$ axis and therefore on the positive $\text{Re}K_1$ axis or

on the positive $\text{Im}K_1$ axis. (There is another on the negative axes which can be important for very strong coupling.) This P -sheet f pole means that in the vicinity f_{eff} will take on all complex values, and all possible $\text{Im}f_{\text{eff}} < 0$ will be on P . $\text{Im}\theta_1^{-} \geq 0$ on P ; therefore in this case by Eq. (16) there is always a P -sheet zero of S_{11} . This is a CDD singularity relevant to a Levinson's theorem for $\arg S$.

When the above f pole is on the $\text{Re}(K_1)$ axis, Eq. (16) shows that there is a pole of S_{11} with $\text{Im}K_1 < 0$ near the f pole. This U_1 -sheet pole of S is, of course, a resonance. If the f pole is on the positive imaginary axis, the S_{11} pole is also on that axis, creating a true bound state.

For very small $f_{1\lambda}$ the above S_{11} zeros and poles will both be very close to the f pole and will merge when $f_{1\lambda} = 0$. Therefore, the emergence of CDD singularities when $f_{\lambda\lambda} < f_c$ is due to their simultaneous creation, at the f pole, with S_{11} poles.

(c) When $f_{\lambda\lambda} > f_c$ the emergence of a CDD pole is entirely different. As the f pole is at $\text{Im}K_{\lambda} < 0$, the zero of S_{11} will also have $\text{Im}(K_{\lambda} < 0)$ when $f_{1\lambda}$ is sufficiently small. When $f_{\lambda\lambda}$ is sufficiently large, then the S_{11} zero is on U_1 , as given by the discussion of Sec. V(a). It only emerges on P when $f_{1\lambda}$ is sufficiently large.

If we specialize to SBCM, $L=0$ state interactions, the condition for an S_{11} zero is

$$f_{11} - \frac{f_{1\lambda}^2}{f_{\lambda\lambda} - iK_{\lambda}r_0} + iK_{\lambda}r_0 = 0. \quad (50)$$

Equation (50) can be used to follow the zero in detail for a variety of cases, but our present purpose is served by the following examples: If both particles in channel i have mass M_i , and

$$\mu^2 = (M_{\lambda}^2 - M_1^2)r_0^2, \quad (51)$$

then

$$K_{\lambda}r_0 = [K_1^2 r_0^2 - \mu^2]^{1/2}. \quad (52)$$

We first assume

$$K_{\lambda}r_0/\mu \ll 1 \quad (53)$$

and obtain from Eqs. (50) and (52)

$$(K_{\lambda}r_0)_0 = -if_{\lambda\lambda} + \frac{f_{1\lambda}^2}{f_{11}^2 + \mu^2}(if_{11} + \mu). \quad (54)$$

Thus K_{λ} becomes real when

$$f_{1\lambda}^2 = \frac{f_{\lambda\lambda}}{f_{11}}(f_{11}^2 + \mu^2), \quad (55)$$

at which value of $f_{1\lambda}$

$$(K_{\lambda}r_0)_0 = f_{\lambda\lambda}\mu/f_{11}, \quad (56)$$

which is consistent with our assumptions if $0 < f_{\lambda\lambda}/f_{11} < 1$. Thus the S_{11} zero emerges onto P , becoming a CDD pole, on the inelastic cut.

²⁸ G. F. Chew and S. Mandelstam, Phys. Rev. **119**, 467 (1960).

²⁹ G. Frye and R. L. Warnock, Phys. Rev. **130**, 478 (1963).

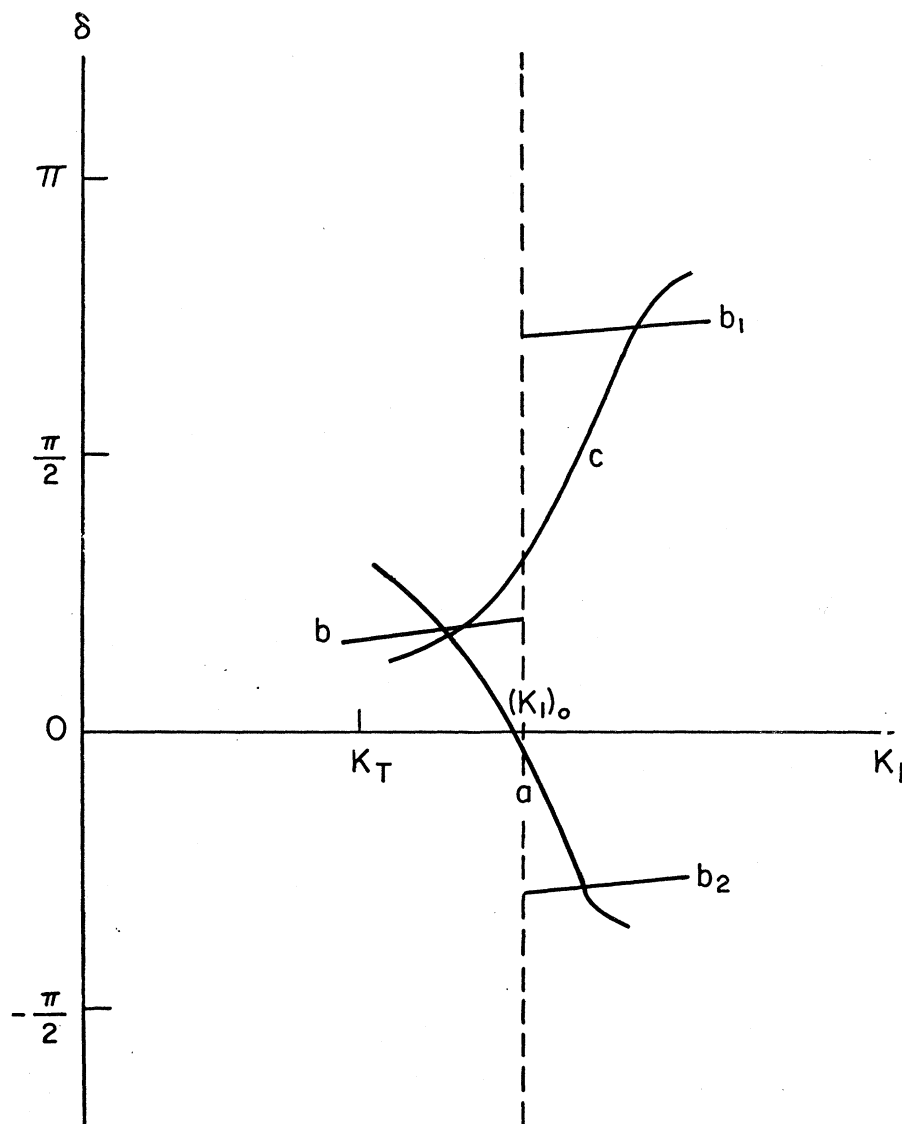


FIG. 3. Behavior of the phase shift on the emergence onto the physical sheet of an S -matrix zero. Curve a represents a typical phase shift curve when the zero is just below the physical cut. Curve b represents the phase shift curve when the zero is on the physical cut (at the phase shift discontinuity). After the zero either b_1 or b_2 may be chosen, since they differ by π and the criterion of continuity is inapplicable. In curve c the zero has moved a small distance into the physical region.

For larger $f_{1\lambda}$, the zero moves into P . If we let $f_{1\lambda}$ become very large then, without condition (53), we obtain

$$(K_{\lambda}r_0)_0 = \pm f_{1\lambda}^2,$$

showing the asymptotic behavior of the S_{11} zero that emerged above, and that of its twin which emerged on the negative $\text{Re}(K_{\lambda})$ axis.

Returning to the condition of Eq. (55) when the zero is just emerging, we study the behavior of the phase shift. We expand

$$K_{\lambda}r_0 = (K_{\lambda}r_0)_0 + \epsilon, \quad (57)$$

$$\eta_{11}e^{2i\delta_{11}} \equiv S_{11} = -\frac{\epsilon}{2K_{\lambda}r_0} \left[1 + \frac{f_{11}^2 + \mu^2}{f_{\lambda\lambda}(1 - i\mu/f_{11})} \right]. \quad (58)$$

Because $\eta_{11} > 0$, it follows that δ_{11} makes a discontinuous

jump by $\frac{1}{2}\pi$ at $(K_{\lambda}r_0)_0$. Investigation of the behavior of Eq. (16) when $f_{1\lambda}^2$ slightly fails or exceeds the criterion of Eq. (55) establishes the picture of Fig. 3. When $f_{1\lambda}^2$ is a little smaller than the critical value, the phase shift has some value δ just before $(K_I)_0$ (in Fig. 3 we pick $\delta \approx \frac{1}{4}\pi$, but this depends on f_{11} , $f_{\lambda\lambda}$, and μ) and then drops rapidly to $\delta_+ = \delta_- - \frac{1}{2}\pi$. When $(f_{1\lambda})^2$ exceeds the critical value, the phase shift rises rapidly through resonance to $\delta_+ = \delta_- + \frac{1}{2}\pi$. At the critical $(f_{1\lambda})^2$ the jump in δ is ambiguously $\pm \frac{1}{2}\pi$. Thus as the CDD zero is brought into the physical region, the difference of the phase shift from elastic threshold to infinite momentum $[\delta(\infty) - \delta(0)]$ increases by π .

It is important to remember that the CDD zero only moves from U to P when $f_{\lambda\lambda} > f_c$ and only then does $\delta(\infty) - \delta(0)$ change. When $f_{\lambda\lambda} < f_c$ as, in Sec. V(b), the CDD pole is always in P for any nonzero $f_{1\lambda}^2$.

When $f_{1\lambda}^2 \rightarrow 0$, the position of the S_{11} zero moves to the boundary of P , but any consequent singularity in δ is cancelled by the simultaneous approach of the S_{11} pole from the unphysical side.

(d) In a finite-channel BCM there is no absolute Levinson's theorem, because $\delta(\infty) - \delta(0)$ is *always* negative infinite. This can be seen from the asymptotic behavior of Eq. (16):

$$\lim_{K_1 \rightarrow \infty} S_{11} \rightarrow -e^{-2iK_1 r_0}. \quad (59)$$

But the above discussion established a *relative Levinson's theorem* for the multichannel BCM:

$$\pi \Delta[\delta(\infty) - \delta(0)] = \Delta[n_c - n_b], \quad (60)$$

where n_c is the number of CDD poles of the present type (S_{11} zeros on the physical sheet), and n_b is the number of bound states. The emergence of a bound state decreases $\delta(\infty) - \delta(0)$ by π in the usual way, i.e., by increasing the phase shift near threshold so that $\delta(0)$ increases discontinuously by π as the bound state emerges.

(e) We shall now establish that for real $f_{\lambda\lambda}$ (the centrally coupled case) A_{11} poles are on the $\text{Re}(K_1)$ axis below inelastic threshold if the f pole is located there, or on the $\text{Im}(K_1)$ axis if $|f_{\lambda\lambda}|$ is large enough to put the f pole there.

Let $K_{\lambda r_0} = i\chi_\lambda$. Let the f pole be at $\chi_\lambda = \chi_P$ and let $-\chi_T < \chi_P < \chi_T$, where $\pm\chi_T$ corresponds to elastic threshold ($K_1 = 0$). Consider the factor $\sigma \equiv (f_{\text{eff}} + \theta_1^-) \times (f_{\text{eff}} + \theta_1^+)^{-1}$ of Eq. (16). Its phase (argument) vanishes at $K_1 = 0$ because the θ_1^\pm are real at that point. Its phase also vanishes at $f_{\text{eff}} = \infty$, where $\sigma = 1$. Thus as χ_λ goes from χ_T to χ_P through 0 and on to $-\chi_T$, the phase of σ must go continuously from $-\pi$ to $\pi \pmod{\pi}$ or from π to $-\pi \pmod{\pi}$, provided the θ_1^\pm are not singular in that region. (If θ_1^\pm are singular anywhere but at χ_P and χ_T , the phase of σ will go through the full range more than once.) It follows that the phase of σ will cancel the phase of J_1^-/J_1^+ in $S_{11} = \sigma J_1^-/J_1^+$, somewhere in the interval $-\chi_T < \chi_\lambda < \chi_T$, because the latter factor depends on K_1 only (and therefore not on the sign of χ_λ). Let the cancellation take place at $\chi_\lambda = \chi_0$. Since $|S_{11}| = 1$ in the whole interval, it follows that $S_{11} = 1$ and $A_{11} = 0$ at χ_0 . This A_{11} zero will be physical (unphysical) if χ_0 is positive (negative). If $f_{1\lambda}$ is sufficiently small, χ_0 will have the sign of χ_P .

As $-f_{\lambda\lambda}$ or $|f_{1\lambda}|$ increase, the A_{11} zero will emerge onto the physical sheet at the inelastic threshold and move down the elastic cut. Since $\eta = 1$ on the elastic cut, the phase shift $\delta_{11} = 0 \pmod{\pi}$ at the A_{11} zero. The phase $2\delta_{11}$, of S_{11} , is continuous at the A_{11} zero, but the phase ϕ_{11} of A_{11} must jump by π , to accommodate the change of sign of $A_{11} \equiv |A_{11}| e^{i\phi}$. Thus as soon as the zero of A_{11} enters the physical region there is a $\Delta\phi_{11} = \pi$, establishing an extended relative Levinson's theorem for ϕ_{11} . However, since ϕ_{11} remains discontinuous (as the zero moves

down the real axis), this jump of π is wholly artificial. It never turns into a continuous change that would bring ϕ_{11} through $\frac{1}{2}\pi$, or otherwise directly relate to an important structure in the cross section. On the other hand, the resonance associated with the emergence of the S_{11} zero (see Fig. 3) would move into the elastic region with increasing $f_{1\lambda}$, and is not far above the A_{11} zero in most cases.

The case $|\chi_P| > \chi_T$ is probably of less practical interest. However, one can easily show that in this case there will be an A_{11} zero on the positive imaginary K_1 axis. When $\chi_\lambda = \pm\chi_T$, then $\chi_1 = 0$, $\theta_1^\pm = 0$ and $J_1^-/J_1^+ = 1$, so that $S_{11} = 1$ (these kinematic zeros of A_{11} are, of course, always present). When $\chi_\lambda = \pm\infty$ then $f_{\text{eff}} = f_{11}$, $\chi_1 = \pm\infty$, $\theta_1^\pm = \pm\infty$, and $J_1^-/J_1^+ = \infty$, so that $S_{11} = -\infty$. We further note that as χ_λ goes from χ_P to $\pm\infty$, f_{eff} goes smoothly from $-\infty$ to f_1 while θ_1^+ goes smoothly from some finite value to $+\infty$. Therefore, $f_{\text{eff}} + \theta_1^+$ vanishes in the interval, and S_{11} has a pole at that point. At the pole, $f_{\text{eff}} = -\theta_1^+$; and near the pole,

$$S_{11} = \frac{-\theta_1^+ + \theta_1^- J_1^+}{f_{\text{eff}} + \theta_1^+ J_1^+} = \frac{2\chi_1}{(J_1^+)^2} \frac{1}{f_{\text{eff}} + \theta_1^+}, \quad (61)$$

where we have used Eq. (20). As χ_1 proceeds from the S_{11} pole to ∞ , the factor $f_{\text{eff}} + \theta_1^+$ becomes positive. It follows that $S_{11} \rightarrow +\infty$ for χ_1 just larger than the position of the pole. Consequently, between $\chi_1 = \infty$ and the position of the S_{11} pole there is a point at which $S_{11} = 1$, and an A_{11} zero is produced. The A_{11} zero will be on the P sheet if $\chi_P > 0$, and on the U_1 sheet if $\chi_P < 0$.

In this case, when the A_{11} zero is on the P sheet it is always associated with a P -sheet pole—a bound state. In this case $\Delta n_c = \Delta n_b$, and the relative Levinson's theorem for the phase ϕ_{11} applies. (There is no jump in ϕ_{11} at $K_1 = 0$, because the A_{11} pole and the A_{11} zero enter the region $\chi_1 > 0$ simultaneously: $\theta_1^+ = \theta_1^- = 0$ at $\chi_1 = 0$, so that there are cancelling poles and zeros when $f_{\text{eff}} = 0$ at $\chi_\lambda = \chi_T$.)

(f) Complex f poles arise when there are chain-linked channels, as given by Eqs. (34) and (35). As shown by Eq. (22), the $\text{Im}\theta^+(K) < 0$ when $K > 0$. From Eq. (35) it then follows that if $\text{Im}f_{i+1, i+1, \text{eff}} \leq 0$, then $\text{Im}f_{i, i, \text{eff}} < 0$. Beginning with $f_{NN, \text{eff}}$ [Eq. (36)], it follows that $\text{Im}f_{ii, \text{eff}} < 0$ for $i = 2, \dots, N-1$. From Eq. (34) we then have $\text{Im}f_{\text{eff}} < 0$ for $K_1 > 0$, provided one of the K_i ($i \geq 2$) is positive. If we are below threshold for all $N \geq 2$, then f_{eff} is real, as for centrally linked channels.

The important new feature is that $f_{22, \text{eff}}$ may be complex (with negative imaginary part) even if K_2 is pure imaginary for which θ_2^+ is real. It follows from Eq. (34) that f_{eff} has poles for complex values of K_2 , with $\text{Im}K_2 < 0$. [As proven after Eq. (27), $\text{Im}\theta_2^+ < 0$ for $\text{Im}K_2 > 0$, and there can be no poles of f_{eff} in the upper half K_2 plane.] Thus complex f poles are always on the U_1 or U_3 sheets.

For very small f_{12} , f_{eff} will attain all values in a close neighborhood of the f pole. This implies that for sufficiently small f_{12} , there will be S_{11} and A_{11} poles and zeros near the position of the f pole. Thus for weak coupling the zeros as well as the poles will all be on the U_1 or U_3 sheets. As contrasted with cases (b)–(e) above, for any zeros to emerge onto the P sheet the coupling has to be sufficiently large. We will not here follow the movement of the zeros (with increases of f_{12}) to make quantitative estimates of their emergence to the P sheet. But one expects that the zeros will migrate to the right of the threshold branch points of all the chain-linked channels j , for which $j < i$, where channel i has $K_i > 0$ at the f pole.

In Ref. 30, only real CDD poles (with reference to amplitude zeros) are postulated, as being related to coupling to elementary particles. We see here that complex zeros of the amplitude may be expected for the physical case when the coupled elementary particle (or two-particle channel) is itself coupled to some third system and is therefore unstable. The use of dispersion relations for inverse amplitudes is therefore open to important errors.

(g) Since the phase shift $\delta_L = \frac{1}{2} \text{Im} \ln S_L$, it has branch points wherever S_L has a branch point, a pole, or a zero. Consequently, a dispersion relation for δ_L has the form ($\nu = K^2$)

$$\text{Re} \delta_L = \int_{-\nu_L}^{-\infty} d\nu' \frac{f(\nu')}{\nu' - \nu} + \int_0^{\infty} d\nu' \frac{\sigma(\nu')}{\nu' - \nu} + \int_C d\nu' \frac{q(\nu')}{\nu' - \nu}, \quad (62)$$

where the first contribution is from the left-hand cut (ν_L is determined by the lowest mass in the t channel, i.e., the range of the force), the second contribution is that of the physical cut starting at elastic threshold, and the last contribution is that of the complex cuts with branch points at the zeros of S_{11} . In Ref. 12 pion-nucleon phase shifts are computed ignoring the third contribution. The results of Secs. V(b) and V(c) show that the complex cuts being ignored may have branch points within or close to the physical region of interest in Ref. 12. These contributions can therefore invalidate the quantitative results of that reference. In particular, for the S_{11} , P_{11} , and D_{13} , D_{15} , and F_{15} pion-nucleon states there is evidence both in the data³¹ and from model fits to the data^{5-8,10} that coupling to other baryon-meson channels is strong and causes P -sheet S_{11} zeros in several of those cases.

In an attempt to measure the magnitude of effect of inelasticity on the real phase shift, it was conjectured in Ref. 11 that one could ignore the *change* in discontinuities along all cuts except the direct effect of $\text{Im} \delta_L$

on the inelastic part of the physical cut. This leads to

$$\Delta \text{Re} \delta_L(\nu) \approx \int_{\nu_T}^{\infty} \frac{\text{Im} \delta_L(\nu')}{\nu' - \nu}, \quad (63)$$

where ν_T is at the inelastic threshold, and $\text{Im} \delta_L^+ = \frac{1}{2} \ln \eta_{11}$.

Equation (62) is supposed to be a measure of the energy dependence of $\delta_L(\nu)$ introduced by the inelasticity. Using experimental values of η_{11} , it was estimated in Ref. 12 that inelasticity played a relatively small role in the vicinity of the D_{13} resonance. However, this estimate can only be useful when P -sheet S_{11} zeros are absent or remain far away from the physical region of interest. When the S_{11} zeros are present, they move rapidly with the strength of coupling [see Secs. V(b) and V(c)] and therefore also contribute strongly to $\Delta \text{Re} \delta_L$ and its energy dependence.

The approximate position of the branch point on emergence of the S_{11} zero is given by Eq. (56). This leads to an energy dependence over a range consistent with that of Eq. (4) deduced in a model-independent way. The effective masses μ in Eqs. (4) and (56) do not have the same meaning, but both are approximately one to several pion masses.

It follows that the large effects credited to inelasticity by the models of Refs. 6–8 are consistent with analyticity and the resulting dispersion relations for phase shifts when completed by the cuts arising from S_{11} zeros. Results of Refs. 11 and 12 are not reliable when channel coupling is moderately strong, or in the case of quasi-bound-type coupling.⁴

VI. MACDOWELL SYMMETRY IN THE SIBCM

The MacDowell symmetry relation,¹⁹ based on the field-theoretical symmetry under Schwinger space-time reflection, relates odd- and even-parity partial waves with the same J and T of the pion-nucleon system.

$$A_{(L+1)^-}(W) = A_{L^+}(-W), \quad (64)$$

where L^\pm implies $J = L \pm \frac{1}{2}$.

When the analyticity of A_L is sufficient to connect W with $-W$ for physical values of W , then Eq. (64) is, in principle, a powerful relation between the two partial waves. Mandelstam analyticity in the finite plane, such as we have in the BCM, is of course sufficient.

But in applying Eq. (64) there are grave doubts about its utility because of the large extrapolation distance in the W plane. A small difference between the model and actual amplitudes in one region may extrapolate to a very large difference in the other region. In order to connect even the elastic threshold of the two partial waves,¹⁵ the equation spans 2 BeV. This implies that the physical region of one of the partial waves must be accurately represented by a model over several BeV (which includes the inelastic cuts of many channels)

³⁰ S. C. Frautschi, *Regge Poles and S-Matrix Theory* (W. A. Benjamin, Inc., New York, 1963), p. 30.

³¹ A. Donnachie, R. G. Kirsopp, and C. Lovelace, *Phys. Letters* **26B**, 161 (1968).

if the same model parameters are to be of value in the other physical region.

It was with some surprise, therefore, that it was found¹⁵ that the MacDowell reflection of a two-channel SBCM for the $T=\frac{1}{2}$, S -wave πN amplitude gave a qualitative understanding of the $T=\frac{1}{2}$, $J=\frac{1}{2}$ P -wave amplitude. Similar unexpected success of the relation has been found in the connection of the F_{15} and D_{15} πN partial waves.³² It seems worthwhile to extend the results of Ref. 15, and to note some general relations, in case the symmetry proves useful for more detailed models, and in other partial waves.

The extension of the results of Ref. 15 to the multi-channel SIBCМ is very easy. Equation (64) implies the same relations as in Eqs. (6) and (7) of Ref. 15 between the S_L . In Refs 15 and 19 the noncovariant amplitude

$$\mathfrak{F}_{L(+,-)} = (2/W)A_{L(+,-)}$$

was used. Hence Eq. (64) differs by a minus sign from the equivalent equation for the $\mathfrak{F}_{L(+,-)}$. We need only use the property of the Jost functions given by Eq. (18) for K real or imaginary to reproduce the results of Ref. 15, as follows.

(i) If on continuing from physical $W \rightarrow -W$, we reach the sheet $K_1 \rightarrow K_1$, then, using S_R for the MacDowell reflection of S_{11} , we have [by Eq. (64)]

$$S_R(W) = -S_{11}(-W) + 2. \quad (65)$$

Also, $f_{\text{eff}}(-W)$ is real in the elastic region whether we choose the branch $K_i \rightarrow \pm K_i$ ($i \neq 1$). It follows as before that $|S_R(W)| > 1$ in the elastic region and unitarity is violated. Therefore, $K_1 \rightarrow K_1$ is not the continuation on the physical sheet.

(ii) If, corresponding to physical $W \rightarrow -W$, we choose $K_1 \rightarrow -K_1$, then Eq. (64) implies

$$S_R(W) = S_{11}(-W), \quad (66)$$

while at the same time above inelastic threshold (K_i real for some $i > 1$)

$$f_{\text{eff}}(-W) = f_{\text{eff}}(W) \quad \text{if } K_i \rightarrow K_i \quad (67)$$

or

$$f_{\text{eff}}(-W) = f_{\text{eff}}^*(W) \quad \text{if } K_i \rightarrow -K_i \quad (68)$$

using Eq. (18). Equations (66) and (67) together with Eq. (16) imply that $|S_R| > 1$, because the imaginary parts of $f_{R \text{ eff}}$ and θ_1^- add while those of $f_{R \text{ eff}}$ and θ_1^+ subtract. Similarly, Eqs. (66) and (68) together with Eq. (16) imply $|S_R| < 1$.

Consequently, in the SIBCМ the continuation on the physical sheet of $W \rightarrow -W$ implies $K_i \rightarrow -K_i$ for all i . This extends all the formal results of Ref. 15 to the SIBCМ.

It is also easy to extend the threshold condition of Ref. 15 to the SIBCМ parameters. In general at thresh-

old, when $W \approx M_{1A} + M_{1B}$,

$$A_{L^+}(-W) = O(K_1^{2L+1}), \quad (69)$$

so that the amplitude obtained from MacDowell symmetry by Eq. (64)

$$A_{(L+1)^-R} = O(K_1^{2L+1}). \quad (70)$$

Thus in order for $A_{(L+1)^-}$ to have its proper threshold behavior $O(K_1^{2L+3})$, the SIBCМ parameters must be such that the leading term of Eq. (70) vanishes. This implies, using Eq. (16), that the boundary condition and potential parameters are constrained such that

$$f_{L^+}(-K_i^T) = \lim_{K_1 \rightarrow 0} K_1 \frac{(d/dr_0)[J_{L^+}(-K_1) - J_{L^+}(-K_1)]}{J_{L^+}(-K_1) - J_{L^+}(-K_1)}. \quad (71)$$

Conversely, if we obtain the amplitude $A_{L^+}(W)$ by MacDowell reflection of $A_{(L+1)}(W)$, i.e., let $W \rightarrow -W$ in Eq. (64), then in general at the threshold we will obtain

$$A_{L^+R}(W) = O(K_1^{2L+3}). \quad (72)$$

To restore A_{L^+R} to its proper K_1^{2L+1} behavior at threshold, the model parameters are constrained to make the coefficient of the leading term infinite:

$$f_{(L+1)^-}(-K_i^T) = -\theta_{(L+1)^+} \quad (K_1 = 0). \quad (73)$$

In addition to the above extensions of the results of Ref. 15, we note here a simple relationship that always holds between an SIBCМ amplitude and its MacDowell reflection when above the thresholds of all the coupled channels. Under that condition, all the K_i are real and Eqs. (18), (66), and (68) together show that

$$S_R(W) = S_{11}^*(W), \quad W > \text{all thresholds} \quad (74)$$

from which it follows that

$$\eta_{(L+1)^-} = \eta_{L^+} \quad (75)$$

and

$$\delta_{(L+1)^-} = -\delta_{L^+} \quad (76)$$

when W is greater than all thresholds.

The utility of this result is severely put in question by the expectation that there is no upper limit to the threshold mass of coupled channels. Practically, however, where there is a sufficiently large gap between thresholds the relation may be expected to hold approximately just above the lower of the two thresholds. The empirical approximate ratification of this condition is a necessary condition for the applicability of MacDowell symmetry to a finite coupled-channel model; i.e., conditions (75) and (76) should be approximately satisfied just above the highest model threshold.

In the CERN phase-shift analysis³¹ the above conditions are qualitatively obeyed near the ρ production threshold for the S_{11} - P_{11} and the D_{15} - F_{15} pairs of partial waves. This indicates that the calculation of Ref. 15

³² S. Hirschi and E. Lomon (private communication).

should be expanded to include the ρN and ωN channels as well as ηN and σN channels. Recently,³² it has been shown that the D_{15} resonance can be obtained by a MacDowell reflection of an SBCM description of the F_{15} resonance, in which the πN and ρN channels are coupled.

The above discussion generalizes to the SIBCM the formal results proven previously for the SBCM only.¹⁵ Moreover, it explains the approximate success of previous SBCM applications to MacDowell symmetry,^{15,32} recognizing that $\theta_L(\pm K) \rightarrow {}^H\theta_L(\pm K)$ for large K . An SBCM amplitude with parameters fitted to large K data will, on MacDowell reflection, give an accurate prediction for large $|K|$, if the important channels are included. The unphysical cuts of the SIBCM will only become important at small $|K|$, where they will certainly modify the threshold conditions.

VII. BEHAVIOR IN THE ANGULAR MOMENTUM PLANE

The first application of the BCM to exploration of singularities in the angular momentum plane was made by Gribov and Pomeranchuk.²⁰ Using the energy independence of \mathfrak{f}_L (called $\chi_{L+1/2}$ in Ref. 20) for small momenta, and assuming that \mathfrak{f}_L has no singularity as a function of L for $L = -\frac{1}{2}$, they establish the existence of an accumulation of an infinite number of poles at $\text{Re}L = -\frac{1}{2}$ at any two-body threshold. They extend this to the existence of similar accumulations of poles on lines $\text{Re}L = -\frac{1}{2}(3n-5)$ at any n -particle threshold.

The relevance of the model to understanding analytic structure in the L plane extends to many other aspects

than the above. In Sec. VII(a) we examine the leading Regge trajectories for small momenta, obtaining explicit relations between the value and the slope at a two-particle threshold. Section VII(b) contains the most interesting results. In it, it is shown that the infinite-channel, asymptotic-energy condition of Sec. IV, leads to asymptotically rising Regge trajectories. The rate of rise is consistent with Mandelstam analyticity.³³ The W^2 behavior observed at presently available experimental energies is not asymptotically consistent with the Mandelstam assumption. In Sec. VII(c) we note that multiparticle channels (\geq three particles) lead to Regge cuts, and explore a few qualitative features of the branch-point trajectories. In each case we shall assume that \mathfrak{f} has no explicit dependence on L .

(a) Neglecting the potential tails (i.e., the SBCM is assumed) the condition for S -matrix poles is easily obtained from Eq. (16) as

$$f_{\text{eff}} + {}^H\theta_1^+(K_1) = 0, \quad (77)$$

with ${}^H\theta_i^+$ defined as in the discussion before Eq. (28). The analytic extension to complex values of L_1 is contained in the well-known analytic extension of the Hankel functions. We can most easily know the position of the pole in the L_1 plane as a function of K_1 near elastic threshold, $K_1=0$. This can be extrapolated back to $W=0$, to the approximation that the linear behavior in K^2 holds in the low-energy range. For $L_1 \leq \frac{1}{2}$ the usual Hankel function expansions are not adequate and one must be careful to reexpress the result in terms of Bessel functions of order $\pm L_1$ and use their expansions. One obtains

$${}^H\theta_{L^+}(K) \approx \frac{L + (L-2)Z^2/2(2L-1) - ie^{-iL\pi}(L+1)\lambda_L Z^{2L+1}[1 - (L+3)Z^2/2(L+1)(2L+3)]}{1 + Z^2/2(2L-1) + ie^{-iL\pi}\lambda_L Z^{2L+1}[1 - Z^2/2(2L+3)]}, \quad (78)$$

where $Z = Kr_0$ and $\lambda_L = \Gamma(-L + \frac{1}{2})2^{-2L-1}\Gamma^{-1}(L - \frac{3}{2})$. For $L > \frac{1}{2}$, the terms proportional to $e^{-iL\pi}$ are of higher order than Z^2 and may be dropped. Inserting in Eq. (77), one obtains for the leading trajectory, assuming $f_{\text{eff}} \approx f_0 + f_1 K^2$ [$f_1 < 0$ is a consequence¹³ of (Eq. 27)],

$$L_p = -f_0 - (1 + 2f_0)^{-1}(1 + 2f_0 f_1 + f_0)Z^2. \quad (79)$$

We note that the condition for bounded asymptotic cross sections in the crossed channel that $L_p^0 \equiv L_p(K=0) \leq 1$ is equivalent to the condition that $f_0 \geq -1$. The latter implies that the system be no more than just bound in the $L=1$ state. To be consistent with the present condition on L , $f_0 < -\frac{1}{2}$. Together with the above condition on f_1 , it follows that the slope is positive as observed for the Regge trajectories with $L_p^0 > \frac{1}{2}$. It is useful to write the slope in terms of L_p^0 :

$$\left(\frac{dL_p}{dK^2}\right)_0 = \frac{1 + f_1(1 - 2L_p^0)}{2L_p^0 - 1} r_0^2. \quad (80)$$

In Eq. (78) one also observes that $\text{Im}{}^H\theta_{L^+} = O(Z^{2L+1})$, from which, as expected,

$$\text{Im}L_p \sim K^{2L_p+1}. \quad (81)$$

When $-\frac{1}{2} < L < \frac{1}{2}$, one observes that the third term of both the numerator and denominator of Eq. (78) dominates over the second term, and consequently

$${}^H\theta_{L^+} = L - ie^{-iL\pi}(2L+1)\lambda_L Z^{2L+1}, \quad (82)$$

from which one again concludes that $L_p^0 = -f_0$. However, the K^2 dependence at threshold is lost, because $(-\frac{1}{2} < f_0 < \frac{1}{2})$

$$L_p \approx -f_0 + e^{i(f_0-1/2)\pi}(1-2f_0)\lambda_{-f_0}(kr_0)^{1-2f_0} \quad (83)$$

and $(dL_p/dK^2)_0$ is infinite. For larger values of K , the K^2 behavior will dominate the K^{1-2f_0} behavior. The transition to the K^2 behavior will take place quickly if L_p^0 is less than but close to $\frac{1}{2}$.

³³ R. W. Childers, Phys. Rev. Letters **21**, 868 (1968).

At $L = -\frac{1}{2}$, the Z^{2L+1} in the denominator of Eq. (78) oscillates as a function of $\text{Im}L$ more and more rapidly as $K \rightarrow 0$. The accumulation of singularities described in Ref. 20 results from that behavior. Consequently, for $f_0 > \frac{1}{2}$, the leading singularities at threshold are at $L = -\frac{1}{2}$.

The leading physical trajectories other than the Pomeranchon have $L_p(W=0) \approx \frac{1}{2}$. Extrapolating them to the elastic threshold of the lightest particle pair on the trajectory, it is expected that $L_p^0 \gtrsim \frac{1}{2}$. Consequently, Eq. (80) applies to these leading trajectories and the slope expected is approximately equal to $(2L_p^0 - 1)^{-1} r_0^2$. If the effective radius of interaction is $\approx 0.2 \text{ BeV}^{-1}$, then the factor $2L_p^0 - 1$ explains the large slope ($\approx 1 \text{ BeV}^{-2}$) of these trajectories. For the Pomeranchon, should it be regarded as a simple Regge-pole trajectory of $L_p^0 \approx 1$, we predict a very small slope $\approx 0.04 \text{ BeV}^{-2}$, as is indicated experimentally.

(b) Although in this subsection we are exploring the behavior of trajectories as $K \rightarrow \infty$, we cannot use the simple asymptotic formulas for the Hankel functions, because for rising trajectories, the condition $Kr_0 \gg L_p$ may not be satisfied. However, we may use Watson's formula³⁴

$$H_p^{(1,2)}[(p^2 + q^2)^{1/2}] \approx \frac{1}{3} q e^{\pm i(\phi + \pi/6)} H_{1/3}^{(1,2)}(Y), \quad (84)$$

in which $H_p^{(1)}$ and $H_p^{(2)}$ are the cylindrical Hankel functions of order p , $Y = q^3/3p^2$, and $\phi = q - \gamma - p \tanh^{-1} \times (q/p)$. The error in Eq. (84) is $< 24p^{-1}$, so that it is valuable for large p , independently of the size of q . Using the relation

$$h_L^{(1,2)}(Z) = (\pi/2Z)^{1/2} H_{L+1/2}^{(1,2)}(Z), \quad (85)$$

one is now able to compute the ${}^H\theta_L^+$ to insert in Eq. (77) for large K_1 .

$$\begin{aligned} {}^H\theta_{p-1/2}^+(Z) &= -\frac{1}{2} - \frac{Z}{H_p^{(1)}} \frac{d}{dZ} H_p^{(1)} \\ &= -\frac{1}{2} + \frac{Z^2}{q^2} \left(\frac{1}{2} + \frac{iq^5}{p^2 Z^2} + 3{}^H\theta_{-1/6}^+(Y) \right). \end{aligned} \quad (86)$$

We now assume, self-consistently as will be seen below, that q/p does not vanish as $Z \rightarrow \infty$, from which it follows that $Y \rightarrow \infty$, and we may use the asymptotic behavior of $\theta_{-1/6}^+(Y) \approx -iY$. We then have

$$\begin{aligned} {}^H\theta_{p-1/2}^+ &\approx -\frac{1}{2} - \frac{Z^2}{q^2} \left(-\frac{1}{2} - \frac{iq^5}{p^2 Z^2} + \frac{iq^2}{p^2} \right) \\ &\approx -i\alpha Z + \frac{1}{2}(1 - \alpha^2)/\alpha^2, \end{aligned} \quad (87)$$

where we have put $q = \alpha Z$, $p = (1 - \alpha^2)^{1/2} Z$, as is consistent with the above assumption concerning p/q if $\alpha \neq 0$.

³⁴ Eugene Jahnke and Fritz Emde, *Tables of Functions* (Dover Publications, Inc., New York, 1945), p. 142.

Using the asymptotic result [Eqs. (45) and (46)]

$$f_{\text{eff}} \approx -iZ - \ln Z \quad (88)$$

together with Eq. (87) in the trajectory condition [Eq. (77)], we have

$$\alpha = -1 + (i/Z) \ln Z, \quad (89)$$

confirming the assumed asymptotic behavior of p/q . It follows that

$$L_p \approx p \approx e^{i\pi/4} (2Z \ln Z)^{1/2}. \quad (90)$$

Thus we predict asymptotically rising trajectories that behave as $(K \ln K)^{1/2}$. The real and imaginary parts are asymptotically equal. This prediction does not rise as quickly as the present extrapolation from experiment ($\sim K^2$) but is consistent with the requirement of Mandelstam analyticity³⁵ that $L_p = O(K)$. On the other hand, it violates the result³³ $(\text{Re}L_p)/(\text{Im}L_p) \rightarrow 0$ obtained under the assumption that the amplitude is asymptotically bounded by a polynomial for unphysical scattering angles. The results of Sec. IV do not require that condition to be met on the total amplitude. Each partial-wave amplitude is asymptotically unity, but for higher L the asymptotic behavior is reached for larger K , and the phase oscillations are always present. The cumulative effects of large- L contributions at unphysical $\cos\theta$ may violate the asymptotic conditions assumed in Ref. 33.

The asymptotic behavior predicted by Eq. (90) is not to be expected to set in until the density of coupled channels is very large. This is not yet so in the present experimental range, so that our result is not inconsistent with the present evidence for $L_p \propto K^2$. However, Eq. (90) does predict an eventual decrease towards zero of the Regge-trajectory slopes (as a function of K^2).³⁵ The equality predicted for the real and imaginary parts of L_p is consistent with the narrow-resonance widths observed in the present energy range. The results of Ref. 33 imply larger widths.

These results are derived formally from the SBCM equations. However, asymptotically the general BCM model reduces to the SBCM, extending these results to the general case.

(c) For any finite number of coupled two-particle channels, the meromorphic properties of f_{eff} introduce only poles and Landau singularities²⁰ into the L plane. This is no longer so if three- (or more) particle channels are introduced. We discussed this case in Sec. III(c) and obtained the result of Eq. (33), which we rewrite

$$f_{\text{eff}} = f_{L_1} - D \int_{M_1}^{\infty} \frac{\rho(M) dM}{f_{L_2(L_1)}(K_2) + \theta_{L_2(L_1)}^+[K_2(M, K_1)]} \quad (91)$$

to emphasize the dependence on L_1 and K_1 . It is clear that the denominator of the integral has a continuously

³⁵ P. J. Kelemen, K. Y. Lee, and W. F. Piel, Jr., *Phys. Rev. Letters* **23**, 998 (1969). This data analysis suggests a changing slope.

moving zero at $L_1=L_0(M,K_1)$ as M varies between M_T and ∞ . Consequently, f_{eff} has a branch point at $L_1=L_0(M_T,K_1)$, the branch-point trajectory being determined by the K dependence of L_0 .

If $\eta(M,K_1)$ is the residue of the pole of the integrand, then an explicit description of the cut trajectory is given by

$$f_{\text{eff}}(K) = f_{L_1} - D \int_{M_T}^{\infty} \frac{\eta(M,K) dm}{L_1 - L_0(M,K)}. \quad (92)$$

Through Eq. (16), the cut trajectory of Eq. (92) is introduced into the amplitude. Equation (91) allows us to examine the position of the branch point. Because channel 1 and channel 2 are coupled to each other when physical, the leading trajectory is given by

$$L_{1,\text{max}} = L_2 + \Delta, \quad (93)$$

where Δ is the sum of the spins of the initial-state particles and the final-state resonances. At inelastic threshold ($K_1=K_T$, $K_2=0$) the denominator of Eq. (91) vanishes at

$$L_2 = -f_2, \quad (94)$$

from which it follows that the branch point in the L_1 plane is

$$L_{b_p}(K_T) = -f_2 + \Delta. \quad (95)$$

Now we examine the position of the produced branch points at elastic threshold, or at $W=0$; K_2 is imaginary, and for large values of M_T , $|K_2| = \chi_2$ is large. We then use the asymptotic expression for ${}^H\theta_{L_2}^+$ and obtain

$$L_{b_p}(0) \approx -\frac{1}{2} + \Delta + i(2\chi_2 \ln \chi_2)^{1/2}. \quad (96)$$

Comparing Eqs. (95) and (96), one sees that

$$\text{Re}[L_{b_p}(\chi_T) - L_{b_p}(0)] \approx -f_2 + \frac{1}{2}. \quad (97)$$

Since f_2 is not expected to diverge with M_T , it can be deduced that coupling to higher-mass multiparticle thresholds gives rise to flatter branch-point trajectories.

We conjecture on the basis of the above qualitative discussion that the L -plane branch-point trajectories near $W=0$ may accumulate (for indefinitely large M_T) to a zero-slope envelope. This effect may replace that of a zero-slope Pomeranchon, leading to asymptotic constant cross section with the cessation of diffraction-peak shrinking. This corresponds physically to the result of black-sphere scattering, which is the classical description of the effect of many open channels.

VIII. CONCLUSIONS

In commenting on the results of this paper we first note that most of them hold for the general BCM or at least for the SIBCM in which long-range interactions are allowed in the diagonal interactions. The validity of the BCM is discussed in Ref. 13. It has recently been given further justification in a particular reaction.²¹

In the general discussions of Sec. II, and also within the various coupling schemes of Sec. III, it has been shown that coupled channels cause important energy dependences in partial waves far below the inelastic threshold, even in the region of elastic threshold. For strong-coupling situations one is led to expect elastic and inelastic resonances to be induced by channel coupling. The validity of the one-channel calculation becomes highly doubtful in most instances.

A counter argument on the importance of inelastic effects has been shown to be based on invalid phase-shift dispersion relations (Sec. V). In the process of identifying the singularities of the phase shifts, detailed information on the CDD poles (amplitude and S -matrix zeros) was obtained. The amplitude zeros invalidate inverse-amplitude dispersion relations.

In Sec. IV it was shown that a reasonable asymptotic density of channel openings would lead to a constant asymptotic behavior of each partial wave. This establishes an important improvement on the results of Ref. 13 (for a finite number of channels) which require an asymptotic essential singularity. This result indicates the futility of asymptotic theorems based on elastic formalisms. Moreover, the partial-wave S matrix vanishes asymptotically, in contrast to the more usual vanishing of the amplitude. Later, in Sec. VII, it was shown that the same infinite-channel condition leads to rising Regge-pole trajectories. We conclude that a valid discussion of the asymptotic behavior of Regge trajectories must include the effect of many-channel coupling.

In Sec. VII we also discussed the effect of coupled channels on Regge pole and cut trajectories at finite energy. Supplementing the results of Gribov and Pomeranchuk²⁰ based on the BCM, we have established several other predictions of the coupled-channel BCM. We qualitatively predict the very different slopes of trajectories passing $W=0$ at $L \approx \frac{1}{2}$ (ρ and ω trajectories) and those which pass at $L \approx 1$. Cuts are shown to arise from multiparticle channels. The behavior of the branch-point trajectories has not been explained in any detail, but some indication has been obtained for a flat envelope to all of them. This would establish the expected physical relation between high absorptivity and a finite diffraction width, if the branch-point contributions asymptotically dominate the Regge poles.

Finally, in Sec. VI we explored the consequences of MacDowell symmetry on BCM amplitudes. It was argued that the coupled-channel effects are more important than the effect of the long-range potential in attaining the symmetry. This justifies some of the past success of the MacDowell symmetry with SBCM amplitudes. We also showed that the symmetry establishes simple relations between the coupled-channel amplitudes for energies sufficiently below higher-mass thresholds.

In conclusion, the importance of coupled channels both at finite energy and asymptotically has been

emphasized. Physical processes, dispersion relations, W -plane and L -plane analyticity are all shown to be strongly affected. In the process the scope and flexibility of the BCM has been greatly enlarged.

APPENDIX

We here establish the unitarity of the S matrix generated by the most general coupled-channel BCM. The potential is of the general nonlocal, nondiagonal form, only constrained by Hermiticity. The boundary condition matrix is real and symmetric, but otherwise arbitrary. Both the boundary condition and the potential may be energy-dependent. The Schrödinger equation and the boundary conditions for the scattering of incoming channel i into outgoing channels j ($i, j=1, \dots, N$) are

$$-\frac{d^2\psi_{ji}(r)}{dr^2} + \sum_{m=1}^N \int_{r_0}^{\infty} dr' U_{jm}(r, r') \psi_{mi}(r') = K_j^2 \psi_{ji} \quad (\text{A1})$$

(the centrifugal term is absorbed into U_{jm}),

$$r_0 \frac{d\psi_j}{dr_0} = \sum_m f_{jm} \psi_{mi}(r_0), \quad (\text{A2})$$

$$\lim_{r \rightarrow \infty} \psi_{ji}(r) \sim \frac{1}{\sqrt{K_j}} [\delta_{ji} e^{-iK_j r} - S_{ji} e^{iK_j r}]. \quad (\text{A3})$$

In Eq. (A1) the nonlocality at r does not extend to $r' < r_0$: For energy-independent f_{ij} it has been established³⁶ that $\psi_{ij} = 0$ for $r < r_0$, automatically imposing the cutoff at r_0 on nonlocal effects. For energy-dependent f_{ij} , the short-range nonlocal effects are to be included in the boundary condition.

We also write the counterpart of the above for ψ_{jn}^* :

$$-\frac{d^2\psi_{jn}^*(r)}{dr^2} + \sum_{m=1}^N \int_{r_0}^{\infty} dr' U_{jm} \psi_{mn}^*(r) = K_j^2 \psi_{jn}^*(r), \quad (\text{A4})$$

³⁶ M. M. Hoenig and E. L. Lomon, Ann. Phys. (N. Y.) **36**, 363 (1966).

$$r_0 \frac{d\psi_{jn}^*}{dr_0} = \sum_m f_{jm}^* \psi_{mn}^*(r_0), \quad (\text{A5})$$

$$\lim_{r \rightarrow \infty} \psi_{jn}^*(r) \sim \frac{1}{\sqrt{K_j}} (\delta_{jn} e^{+iK_j r} - S_{jn}^* e^{-iK_j r}). \quad (\text{A6})$$

Following the usual procedure for unitarity proofs, Eq. (A1) is multiplied by ψ_{jn}^* , Eq. (A4) is multiplied by ψ_{ji} , the second product is subtracted from the first, and the whole expression is summed over j and integrated from r_0 to ∞ . The second derivative term is integrated by parts, and the result is

$$\begin{aligned} \sum_{j=1}^N \left[\psi_{jn}^* \frac{d\psi_j}{dr} - \psi_j \frac{d\psi_{jn}^*}{dr} \right]_{r_0}^{\infty} &= \sum_{j=1}^N \sum_{m=1}^N \int_{r_0}^{\infty} dr \int_{r_0}^{\infty} dr' \\ &\times [\psi_{jn}^*(r) U_{jm}(r, r') \psi_{mi}(r') - \psi_{ji}(r) U_{jm}^*(r, r') \psi_{mn}^*(r')] \\ &- \sum_j K_j^2 \int_{r_0}^{\infty} [\psi_{jn}^*(r) \psi_{ji}(r) - \psi_{ji}(r) \psi_{jn}^*(r)] dr. \quad (\text{A7}) \end{aligned}$$

The first term on the right-hand side vanishes by the Hermiticity of $U_{jm}(r, r')$ while the second term vanishes identically. Substituting Eqs. (A2), (A3), (A5), and (A6) into the left-hand side of Eq. (A7), one obtains

$$\begin{aligned} i \sum_{j=1}^N \lim_{r \rightarrow \infty} [(\delta_{jn} e^{iK_j r} - S_{jn}^* e^{-iK_j r})(\delta_{ji} e^{-iK_j r} + S_{ji} e^{iK_j r}) \\ - (\delta_{ji} e^{-iK_j r} - S_{ji} e^{iK_j r})(\delta_{jn} e^{iK_j r} + S_{jn}^* e^{-iK_j r})] \\ = - \sum_{j=1}^N \sum_{m=1}^N [-\psi_{jn}^*(r_0) f_{jm} \psi_{mi}(r_0) \\ + \psi_{ji}(r_0) f_{jm}^* \psi_{mn}^*(r_0)]. \quad (\text{A8}) \end{aligned}$$

The right-hand side of (A8) vanishes by the symmetry and reality of the \mathbf{f} matrix. On the left-hand side, the terms bilinear in δ and S cancel as do those in δ and S^* . This leaves the equation of unitarity,

$$\sum_{j=1}^N S_{ji} S_{jn}^* = \sum_{j=1}^N \delta_{ji} \delta_{jn} = \delta_{in}. \quad (\text{A9})$$